Article

Physicochemical, Structural, Thermal, and Rheological Properties of Mango Seed Starch from Five Cultivars

Ndahita De Dios-Avila [1], Mario Alberto Morales-Ovando [2,*], Paul Baruk Zamudio-Flores [3], Juan Carlos Bustillos-Rodríguez [4], Magali Ordóñez-García [4], Kati Beatriz Medina-Dzul [5], Teresa Romero-Cortes [6], Jaime Alioscha Cuervo-Parra [6] and Juan Manuel Tirado-Gallegos [7,*]

1   Facultad de Ciencias Agrotecnológicas, Universidad Autónoma de Chihuahua, Av. Universidad S/N Campus 1, Chihuahua C.P. 31310, Mexico; ndedios@uach.mx
2   Facultad de Ciencias de la Nutrición y Alimentos, Universidad de Ciencias y Artes de Chiapas, Libramiento Norte Poniente No. 1150, Tuxtla Gutiérrez C.P. 29039, Mexico
3   Fisiología y Tecnología de alimentos de la Zona Templada, Unidad Cuauhtémoc, Centro de Investigación en Alimentación y Desarrollo A. C., Av. Río Conchos S/N Parque Industrial, Ciudad Cuauhtémoc C.P. 31570, Mexico; pzamudio@ciad.mx
4   Instituto Tecnológico de Ciudad Cuauhtémoc, Tecnológico Nacional de México, Av. Tecnológico # 137, Ciudad Cuauhtémoc C.P. 31500, Mexico; jbustillos@itcdcuauhtemoc.edu.mx (J.C.B.-R.); mordonez@itcdcuauhtemoc.edu.mx (M.O.-G.)
5   Instituto Tecnológico de Conkal, Tecnológico Nacional de México, Av. Tecnológico S/N, Conkal C.P. 97345, Mexico; kati.medina@itconkal.edu.mx
6   Escuela Superior de Apan, Universidad Autónoma del Estado de Hidalgo, Carretera Apan-Calpulalpan Km. 8, Chimalpa Tlalayote S/N, Colonia Chimalpa, Apan C.P. 43900, Mexico; tromerocortes@gmail.com (T.R.-C.); jalioscha@gmail.com (J.A.C.-P.)
7   Facultad de Zootecnia y Ecología, Universidad Autónoma de Chihuahua, Periférico Francisco R. Almada Km. 1, Chihuahua C.P. 31453, Mexico
*   Correspondence: mario.morales@unicach.mx (M.A.M.-O.); jtirado@uach.mx (J.M.T.-G.)

Abstract: Large quantities of seeds are generated and discarded during agro-industrial mango processing. However, mango seeds still contain valuable components such as starch, which has applications in various industries. This study aimed to obtain and characterize starches from the seeds of five mango cultivars (Ataulfo, Manililla, Piña, Tapana, and Tommy Atkins). The isolated starches were evaluated for their physicochemical, morphological, structural, thermal, and rheological characteristics. The starches showed creamy white colorations, and their granules had spherical and oval shapes. This starch source contains a high percentage of apparent amylose, greatly influencing its thermal, rheological, and functional properties. Structural and molecular studies showed that all starches presented an A-type X-ray diffraction pattern, impacting their water absorption and viscosity. The transition temperatures were relatively high, which could be influenced by the length of the amylopectin chains and their intermediate components, the apparent amylose content, and other components such as lipids and anomalous amylopectin. The starches evaluated behaved as pseudoplastic materials, while oscillatory tests revealed that the pastes formed with mango starches are more elastic than viscous. In conclusion, research on the seed starch properties of different mango cultivars provides interesting results for their potential application in foods. It could contribute to the value-added processing of mango seeds as a potential starch source.

Keywords: by-product; mango seed; revaluation; amylose; X-ray diffraction

1. Introduction

Mango (*Mangifera indica*) is a fruit crop grown in tropical regions with great economic value. It ranks third among the perennial crops grown in Mexico, covering an area of approximately 209,576 hectares [1]. Globally, Mexico is fifth in mango production, supplying about 4.3% (2.39 million tons) and having the most significant export share of this fruit in the market [1,2].

This fruit is also called the "king of fruits" because of its taste and high nutritional content; it provides numerous health benefits, so it is consumed fresh or processed [2]. In mango industrialization, only the ripe/unripe pulp is used, from which a wide variety of canned, frozen, dehydrated, or minimally processed foods can be prepared [3]. It is estimated that depending on the variety, between 40% and 60% of the total weight of the fruit is discarded after agro-industrial processing, of which the shell and seed constitute between 12 and 15% and 15 and 20%, respectively [4].

According to official data [1], between 360 and 480 thousand tons of seeds are discarded due to mango pulp processing in Mexico. If these wastes are not properly used, they become a source of environmental pollution due to incineration from methane emissions, leachates, and air pollution [5]. However, these agro-industrial wastes can be used or processed to generate products with commercial value because mango seed contains many nutrients and phytochemicals. Seed composition depends mainly on the cultivar and the different geographical regions that produce this fruit [6]. According to El-Sanafawy et al. [7], the composition of seeds, specifically the kernels (dry matter basis), presents 77% carbohydrates, 6–7% protein, 11% lipids, 2% crude fiber, and 2% ash. Among the components of interest are oil [8], polyphenols [9], phytosterols [10], antimicrobials [11], and starch [12–16].

Starch is a biopolymer composed of amylose and amylopectin. It is isolated from various conventional botanical sources, such as corn (*Zea mays* L.), wheat (*Triticum aestivum* L.), and potato (*Solanum tuberosum* L.) [17–19]. Unfortunately, these crops play an essential role in the human diet as significant energy sources during their intake [20], and their exploitation as sources of starch can negatively impact the food supply chain, compromising food security [21]. For this reason, there is a growing interest in obtaining starch from non-conventional sources, mainly from agro-industrial wastes, such as the seeds of avocado (*Persea americana* Mill.) [22], jackfruit (*Artocarpus heterophyllus* Lam.) [23], loquat (*Eriobotrya japonica*, Thunb.) [24], durian (*Durio zibethinus* Murr) [25], and mango (*Mangifera indica* L.) [26]. Special attention has been paid to revaluing mango seeds of different cultivars (Herein, Tommy Atkins, Ubá, Corazón, Totapuri, Namdokmai, Kaew, and Chokanan). This source stands out from other starches obtained from agro-industrial by-products due to its high yields (27–59%) [27,28], higher lipid content (10.7%) [29], apparent amylose (30–46%) [13,15], and high gelatinization temperature (79–85 °C) [12,29]. These results are supported by those reported in rheological behavior. Kaur et al. [12] and Mieles et al. [30] indicate that the temperature where storage modulus (G′) reached a maximum value for mango seed starch pastes was between 82.1 and 89.4 °C. In this temperature range, the storage modulus (G′ = 44.502 Pa) was higher than the loss modulus (G″ = 14.920 Pa), so the behavior was more elastic than viscous.

In addition, mango starches present small oval granules (~13 μm) [16,31] and a crystalline structure A-type with well-defined peaks at 15, 17, 18, and 23° [15,29,32]. In the short-range molecular order, this source shows the typical signals of a polysaccharide profile with absorption bands between 1155 and 1021 cm^{-1}, where the amorphous and crystalline regions are located [29,30,32]. Although the antioxidant properties of starches have been scarcely researched, Ferreira et al. [27] and Mieles et al. [30] point out that mango seed starches contain bioactive compounds with antioxidant potential, which could potentially be applied in the formulation of food products or other industrial processes. These characteristics may vary depending on the cultivar used, extraction method, fruit maturity stage, and agro-climatological conditions at the source [15,28,33].

Among the possible applications of mango starch, it has the potential to formulate edible coatings for perishable foods such as fresh or dried fruits [28]. These coatings offer adequate protection against lipid oxidation, reduce the rate of respiration and weight loss rate, promote a higher content of phenolic compounds, and inhibit microbial growth. All these effects preserve foods for extended periods to avoid damaging their nutritional quality and commercial value [13,34].

Worldwide, the Tommy Atkins mango is the most studied cultivar for starch isolation due to the commercial importance of its fruits [13,32,35]. However, the morphological,

structural, thermal, and rheological properties of starches depend largely on the type of cultivar, agroclimatic conditions, and fruit maturity [15,31,36]. In Mexico, there is great genetic diversity; this is reflected in the different established mango cultivars (Oro, Manzana, Bola, Machete, Talega, Petacón, Caramelo, Manila, Ataulfo, Tommy Atkins, and Criollo) [37]. Of these, only mango seeds of the Ataulfo, Tommy Atkins, and Criollo cultivars have been explored as a potential source for starch obtention. However, there are limited data about the functional, structural, and rheological properties [38,39]. Therefore, further studies are needed to determine the properties and potential applications of starches obtained from mango seeds. This study aimed to isolate and characterize the physicochemical, morphological, functional, structural, thermal, and rheological properties of native starches isolated from mango seeds of cvs. Ataulfo, Manililla, Piña, Tapana, and Tommy Atkins.

2. Materials and Methods

2.1. Materials

The cultivars used were Ataulfo, Manila, Piña, Tapana, and Tommy Atkins (MA, MM, MP, MT, and MT-A, respectively). Mango fruits of the five mentioned cultivars were harvested at a ripe stage in local orchards in Villa de Acapetahua, Chiapas, Mexico. They were selected for their uniformity in color and size, as well as the absence of spots, mechanical damage, and fungal infection. All chemical reagents used in this research were of analytical grade and were purchased from Sigma-Aldrich (St. Louis, MI, USA).

2.2. Starch Isolation

The ripe mangoes were washed and peeled until the seeds were obtained. The obtained cotyledons were washed with a 6% (v/v) NaClO solution to remove residual pulp. They were then dried at 40 °C for 30 h in a food dehydrator (Parallex, Sacramento, CA, USA) and crushed with an analytical mill (M20, Ika-Werke, Wilmington, NC, USA) until the particles were able to pass through a 150-micrometer sieve (100 mesh). Starch extraction was performed by wet milling, following the methodology of Kaur, et al. [12] with slight modifications. The obtained powders were mixed with 0.05% NaOH solution in a domestic blender (Osterizer, Blender Classic) at maximum speed for 1 min. The obtained dispersion was passed through a 53 μm sieve (270 mesh) to remove impurities. Subsequently, the permeate was re-suspended in 1.5 L of distilled water and then centrifuged (10,000× *g* at 15 °C) for 10 min. The supernatant was discarded, and the non-white layer containing fibers on the starch precipitate was removed (procedure performed in triplicate). Subsequently, the sediment was mixed with distilled water and neutralized with 0.05% hydrochloric acid (HCl). The dispersion was allowed to stand at 25 °C for two hours, and the supernatant was removed by decantation. The solids were washed with absolute alcohol (500 mL) and stirred continuously for 30 min. They were then allowed to stand for two hours, after which the supernatant was discarded. The starch was dried in a convection oven at 40 °C for 24 h. The dried starch was crushed in a mortar. It was then passed through a 150 μm sieve (100 mesh). The final product was sealed in polyethylene bags for subsequent analysis.

2.3. Starch Characterization

2.3.1. Proximal Analysis, Tristimulus Color, and Apparent Amylose Content

Proximate analysis was performed according to AOAC [40] with official methods 934.01 (moisture), 920.39 (fat), 942.05 (ash), and 954.01 (crude protein). The tri-stimulus color was evaluated in quintuplicate with a colorimeter (CR-300, Minolta, Osaka, Japan). Readings were taken according to the CIELAB scale (L*, a*, b*). Apparent amylose content was determined by the iodine colorimetric method reported by Williams et al. [41]. The standard curve was prepared using different ratios of purified amylose and amylopectin. Absorbance was measured at 625 nm in an Evolution 300 spectrophotometer (Thermo Scientific, Waltham, MA, USA).

2.3.2. Scanning Electron Microscopy (SEM)

The size and morphology of the granules of the starch samples were evaluated using an ESEM FEI QUANTA 200 scanning electron microscope (FEI Company, Eindhoven, The Netherlands), according to Gunning et al. [42].

2.3.3. Fourier Transform Infrared Spectrometry (FTIR)

The FTIR spectra of the starches were obtained from 450 to 4000 cm^{-1} with a resolution of 4 cm^{-1} and 34 scans with an infrared spectrophotometer (Spectrum Two, Perkin Elmer, Waltham, MA, USA) with a diamond ATR (attenuated total reflectance) accessory [43]. The baseline of the spectra was corrected from 400 to 1200 cm. The spectra were then deconvoluted employing an average bandwidth of 26 cm^{-1} with a deconvolution factor of 2.4 and triangular apodization. The relative absorbance intensities of the bands at 1022 cm^{-1} and 1047 cm^{-1} were recorded from the baseline. The ratio 1044/1022 cm^{-1} was taken as an indicator of the molecular arrangement (crystallinity index) on the surface of the samples [44].

2.3.4. Thermal Properties

The analysis was carried out using the methodology described by De Dios et al. [22]. The gelatinization transition temperatures (onset, T_o; peak, T_p; and conclusion, T_c) and the change in gelatinization enthalpy (ΔH_{gel}) were obtained by using a differential scanning calorimeter (DSC) model 4000 (Perkin Elmer, Waltham, MA, USA).

2.3.5. X-Ray Diffraction

The crystallinity arrangement of the samples was evaluated with an X-ray diffractometer (Rigaku, model Startlab, Tokyo, Japan) with a Cu-Kα radiation generator and high-speed D/teX detector. Data collection was performed over a 2θ interval from 10 to 40° with a voltage of 40 kV and a current of 44 mA.

2.3.6. Functional Properties

The swelling power (SP) and percent water solubility (%S) of the samples were evaluated at 60, 70, and 80 °C in accordance with the methodology described by De Dios et al. [22]. The following equations were used for the calculations:

$$SP = \frac{Gel\ weight\ (g)}{Sample\ weight\ (g)\ db - Soluble\ weight\ (g)} \tag{1}$$

$$\%S = \frac{Soluble\ weight\ (g)}{Sample\ weight\ (g)\ db} \tag{2}$$

2.3.7. Rheological Properties
Flow Curves

The flow properties were determined using the method described by Sánchez-Rivera et al. [45], with slight modifications. The analyses were conducted with a rheometer AR 1500ex (TA Instruments, New Castle, DE, USA) with a parallel plate geometry (Ø = 60 mm, gap = 1000 µm). Dispersions of each starch (5% *w/w*, db) were prepared in distilled water. The mixture was stirred on a stir plate (PC 420, Corning Inc, Corning, NY, USA) at low revolution for 10 min and then placed on the Peltier heating plate of the rheometer. The parallel plates were covered with a trap sealed with mineral oil to minimize moisture losses in the sample during heating. The rheometer was programmed to heat and cool the sample at a constant shear and heating rate of 50 s^{-1} and 2.5 °C/min, respectively. The sample was first subjected to a heating ramp from 25 to 90 °C and held at this temperature for 10 min. After this time, the sample was cooled down to 60 °C. At this temperature, three consecutive rotational sweeps were performed: the first at a shear rate of 0.06 to 500 s^{-1}, the second from 500 to 0.06 s^{-1}, and the third from 1 to 500 s^{-1}. Finally, the data from the third

rotational sweep were fitted to the power law model $\left(\tau = k\dot{\gamma}^n \right)$ proposed by Ostwal-De Waele. We obtained the flow behavior index (n, adimensional) and the consistency index (k, Pa $\times$ s^n) from this model. All measurements were performed in triplicate.

Viscoelastic Properties

Viscoelastic properties were evaluated in the rheometer and configuration described above, according to the procedure reported by Singh et al. [46]. An aqueous dispersion of 20% (w/w, db) of each starch was prepared in distilled water and stirred for 1 h. The dispersions were placed on the Peltier heating plate of the rheometer at 40 °C. The rheometer was programmed to heat and cool the sample at a constant heating rate of 2.5 °C/min. The samples were first heated from 40 to 90 °C, held at 90 °C for 30 min, and then cooled to 25 °C. The changes in storage modulus (G′), loss modulus (G″), and loss factor (δ) during heating were evaluated within the linear viscoelastic region with a frequency and strain of 1 Hz and 0.5%, respectively. All measurements were performed in triplicate.

2.3.8. Statistical Analysis

The experimental design was completely randomized with a minimum of three replicates per treatment. The results were analyzed using a one-way analysis of variance (ANOVA) with Statistical Minitab® 18.1 software (SCIENTEC, State College, PA, USA). The comparison of means was carried out by the Tukey test ($\alpha = 0.05$).

3. Results

3.1. Yield, Proximal Analysis, Color, and Apparent Amylose Content

The results for the yield and physicochemical composition of starches from mango seeds of different cultivars are presented in Table 1. The starch extraction process yielded 28.70–43.02%, showing significant differences ($p < 0.05$) among the sources evaluated. MT-A starch (43.02%) was the highest yielding source ($p < 0.05$), followed by MA, MT, MP, and MM (41.27, 35.07, 32.25, and 28.70%, respectively). Overall, these results are within the range of what has been reported for mango seed starches from Bagenpalli, Sindhoori, Tommy Atkins, Corazon, Uba, and Totapuri cultivars (27–59%) [27,29,30]. However, based on our results (Table 1), we highlight that the seeds generated during the processing of Tommy Atkins and Ataulfo mangoes could be the best candidates for exploitation as a source of unconventional starch.

Moisture contents ranged from 4.82 to 5.36%. These results are lower than those reported by other authors for starches from mango seed cultivars Tommy and Herein (6–10%) [15,27,35]. In this regard, Tesfaye et al. [47] indicated that the moisture content should be sufficiently low (5.68%) to avoid the growth of microorganisms that degrade starch during storage.

Seed starches from MA, MT, MT-A, MM, and MP showed significant differences in apparent amylose contents of 47.58, 35.79, 32.62, 31.68, and 25.65%, respectively. However, they can be classified as high amylose starches. These results agree with those reported by Souza et al. [15] and Rodrigues et al. [13] for cv. Tommy Atkins mango starch (46.7 and 30.4%, respectively). A wide variation in the amylose content in mango seed starch has been reported in the literature between different cultivars and even within the same cultivar (Tommy, Totapuri, Bagenpalli, Kaew, Chausa, Kuppi, Langra, and Dashehari) [13,15,39,48]. In general, MT starch was the starch with the highest amylose content; this source could have the ability to form firmer and more resistant gels. Therefore, the food industry could use this attribute as a thickening and binding agent [49].

Protein (0.77–0.84%) and lipid (0.10–0.54%) contents were relatively low, showing significant differences among the five mango cultivars. In this regard, Souza et al. [15] observed higher lipid and protein percentages in starch cv. Tommy Atkins (4.63 and 3.63%), which was extracted by wet milling using water as a solvent. These differences can be attributed mainly to the extraction method and salt solutions (NaOH, $Na_2S_2O_5$, and NaHSO$_3$), because these promote better protein solubilization and lipid elimination [48].

These results suggest that the starches obtained have high purity due to their low ash, protein, and lipid content [50].

Table 1. Yield and physicochemical properties of mango seed starches.

Parameter	Cultivar				
	MA	**MM**	**MP**	**MT**	**MT-A**
Yield (%)	41.27 ± 0.66 [a,b]	28.70 ± 0.30 [c]	32.25 ± 0.23 [c]	35.07 ± 0.63 [b,c]	43.02 ± 0.49 [a]
Moisture (%)	4.98 ± 0.48 [a]	5.15 ± 0.37 [a]	5.00 ± 0.10 [a]	5.36 ± 0.03 [a]	4.82 ± 0.04 [a]
Proteins (%)	0.77 ± 0.00 [b]	0.84 ± 0.00 [a]	0.84 ± 0.00 [a]	0.83 ± 0.00 [a]	0.80 ± 0.03 [a,b]
Lipids (%)	0.54 ± 0.02 [a]	0.54 ± 0.04 [a]	0.26 ± 0.01 [b]	0.23 ± 0.01 [b]	0.09 ± 0.07 [b]
Ash (%)	0.40 ± 0.05 [a,b]	0.50 ± 0.04 [a]	0.13 ± 0.04 [b]	0.14 ± 0.06 [b]	0.16 ± 0.09 [b]
Apparent amylose (%)	47.58 ± 1.40 [a]	31.68 ± 0.37[c]	25.62 ± 0.30 [d]	35.79 ± 0.37 [b]	32.62 ± 0.37 [b,c]
Color					
L*	90.54 ± 0.90 [a]	93.37 ± 0.72 [a]	93.56 ± 0.72 [a]	92.01 ± 0.87 [a]	91.53 ± 0.48 [a]
a*	0.38 ± 0.01 [a]	0.36 ± 0.01 [a]	0.24 ± 0.00 [b]	0.27 ± 01 [b]	0.19 ± 0.01 [c]
b*	10.68 ± 0.23 [a]	8.74 ± 0.13 [b]	7.18 ± 0.15 [c]	9.49 ± 0.29 [b]	11.59 ± 0.15 [a]
Particle size (μm)	19.14 ± 0.36 [a]	15.91 ± 0.31 [b]	16.56 ± 0.37 [b]	16.39 ± 0.32 [b]	16.95 ± 0.32 [b]

Values represent the mean ± standard error. Means in the same line with different superscript letters (a–d) are statistically different ($p \leq 0.05$). Cultivars: Ataulfo (MA), Manililla (MM), Piña (MP), Tapana (MT), and Tommy Atkins (MT-A).

All sources evaluated presented a creamy white starch coloration, with lightness values (L*) between 90.54 and 93.56. These results contradict those observed by Souza et al. [15], who suggest that the mango cultivar Tommy Atkins starches present a light brown coloration. On the other hand, Rodrigues et al. [13] report low lightness values (82.6) in the same cultivar, with a negative value in a*(-1.23) and positive in b* (13.5), highlighting a yellowish color; this characteristic is mainly attributed to the synthesis of carotenoids in the seed, with this being a natural colorant. Starch color is an important quality attribute; a high whiteness value suggests low protein and pigment content. This physical parameter significantly influences the industrial uses of starch in the food, pharmaceutical, and agricultural industries, among others [51].

3.2. Morphology and Particle Size of Starch Granules by Scanning Electron Microscopy (SEM)

Figure 1 shows the micrographs obtained by SEM analysis. Starch isolates from MA, MM, MP, MT, and MT-A showed spherical to oval-shaped granules of varying sizes. These results are consistent with those reported for mango seed starch granules from other cultivars [13,15,27]. Generally, smaller granules were spherical, while oval granules presented larger sizes [48]. According to Cordeiro et al. [32], spherical and oval shapes require less mechanical energy during processing, which results in higher water retention. In all cultivars evaluated, it was observed that the granules present smooth surfaces [16]. However, in some granules, it is possible to observe grooves or pore spaces, as in MA, MP, and MT-A starches, which are probably caused by the extraction method, especially during milling after the isolation process [16,29]. These characteristics have also been observed in other starch sources, such as jackfruit seed, corn, wheat, and potato, which may impact their thermal, functional, and digestibility properties [18,52].
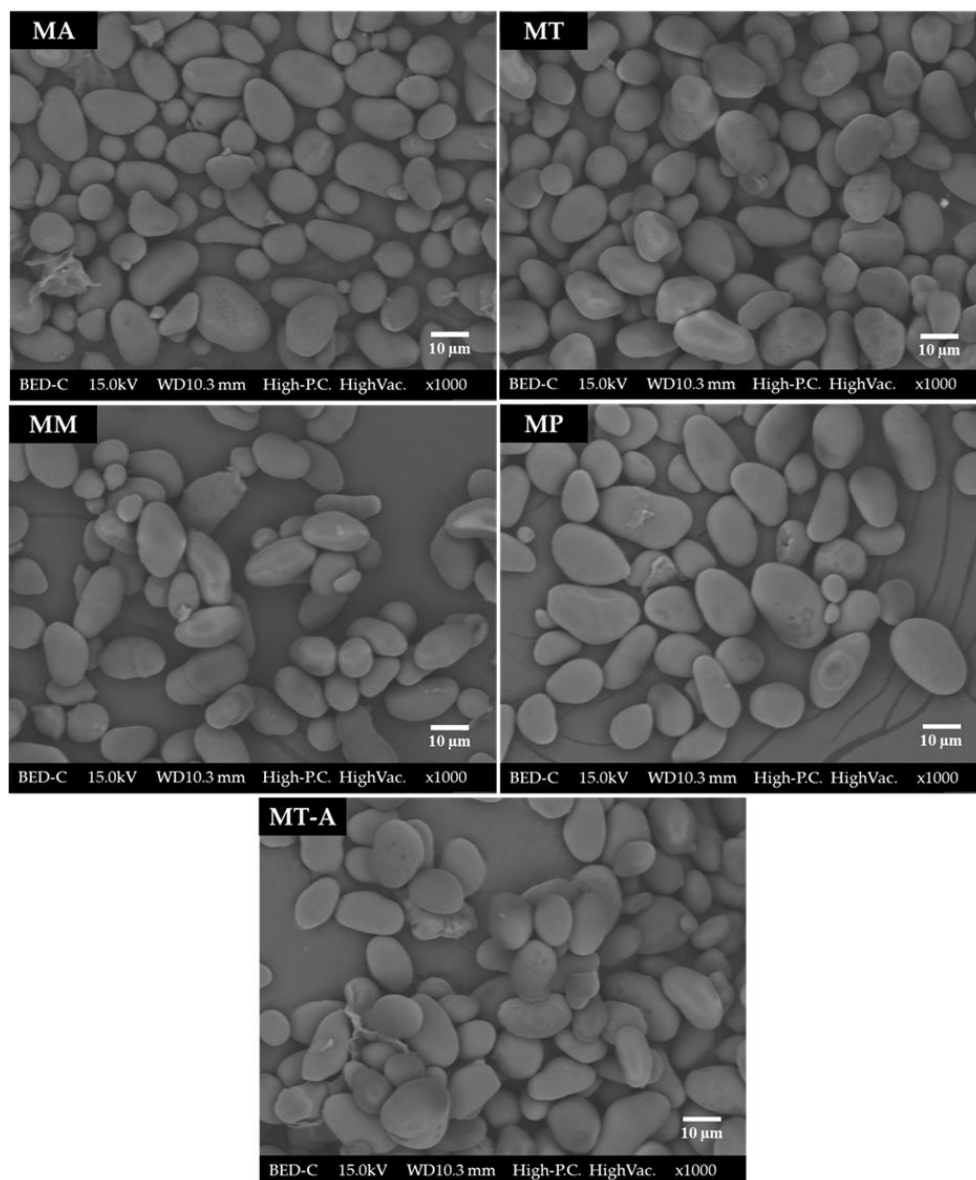
Figure 1. Scanning electron micrographs of mango seed starches. Cultivars: Ataulfo (MA), Manililla (MM), Piña (MP), Tapana (MT), and Tommy Atkins (MT-A).

Table 1 shows the average particle size, showing significant differences ($p < 0.05$) between the sizes of the sources evaluated. MA starch granules presented the largest average size of 19.1 μm, while in the rest of the sources, there were no differences between MT-A (16.9 μm), MP (16.5 μm), MT (16.3 μm), and MM (15.9 μm). These values are within the range observed by other authors for mango starches from different cultivars (7–28 μm) [27,29,31]. Granule size is an important factor during the gelatinization process of starches [39]. According to Rodrigues et al. [13], the size of starch granules affects the way particles interact during different transformation processes. For example, the homogenization process of starch-rich foods is facilitated by smaller starch granules.

3.3. Fourier Transform Infrared Spectrometry (FTIR)

The deconvoluted spectra (800 to 1200 cm^{-1}) of mango starches are shown in Figure 2. In general, all FTIR spectra were similar in all samples evaluated. Within the fingerprint region (400–1200 cm^{-1}), intense peaks characteristic of carbohydrates were recorded, showing no apparent structural differences in the low-range molecular order [53]. The bands 1047 and 1022 cm^{-1} correspond to the crystalline (amylopectin) and amorphous

(amylose) zones, respectively. Ferreira et al. [27] and Ferraz et al. [29] identified signals at 1077, 1067, 1047, 1022, 994, and 930 cm^{-1} in cvs. Tommy and Uba mango starches, which they attributed to deformations of the C-OH and CH2 bonds.
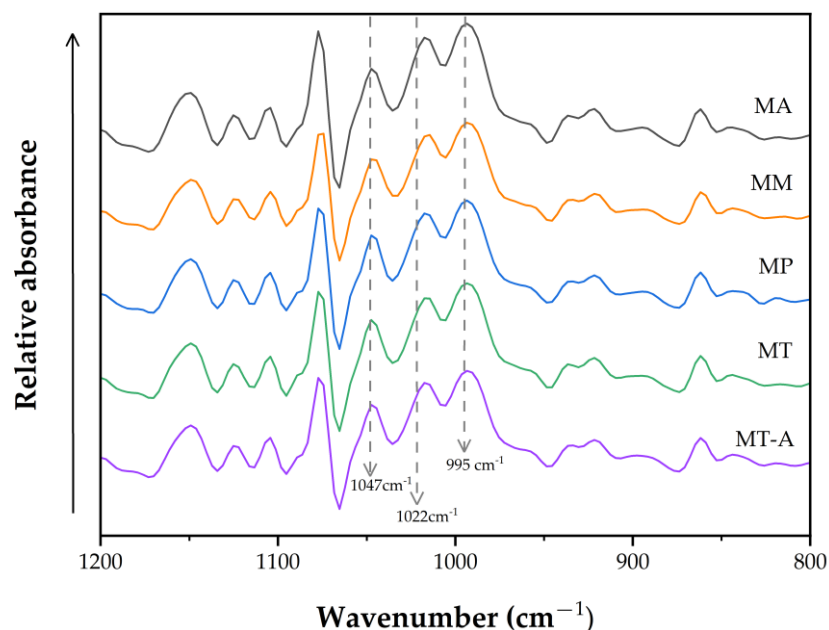

Figure 2. Deconvoluted FTIR spectra of mango seed starches. Cultivars: Ataulfo (MA), Manililla (MM), Piña (MP), Tapana (MT), and Tommy Atkins (MT-A).

The ratio between the bands 1047 cm^{-1} and 1022 cm^{-1} is used to characterize the molecular order and structure of double helices in the short range (Figure 3). Thus, if the ratio is higher, a great amount of ordered structure is present in the external region of the starch granules with an A-type crystallinity pattern [54]. In the present study, MA (1.01), MP (0.97), MT (1.01), and MT-A (0.97) starches presented the highest crystallinity index ($p < 0.05$), with no statistical differences among them, while MM starch (0.9) presented the lowest crystallinity index ($p < 0.05$). These values agree with Ferreira et al. [27] for Tommy Atkins mango starch, with a value of 0.90 for the ratio 1074/1022 cm^{-1}. However, these values are higher than those reported for conventional starch sources such as corn and tubers [17,19] and non-conventional such as avocado seed (0.63) [22]. These results suggest that the starches evaluated in the present research have a higher degree of molecular order in their structures; in this sense, such molecular organization influences some functional properties related to water absorption and viscosity; this characteristic is closely related to XRD patterns [55]. Therefore, a high absorbance ratio of 1047/1022 cm^{-1} values could be interpreted as a high resistance to breaking the starch granule structure by enzymatic hydrolysis or heat treatment, which could impact the gelatinization process.

On the other hand, the ratio 1022/995 cm^{-1} has been used to indicate the characteristics of more hydrophilic materials [55]. The mango starches that showed the highest ($p < 0.05$) affinity for water were MM (0.82), MP (0.81), and MT-A (0.81), with no significant differences between them. In contrast, the MA and MT starches (0.78 and 0.77, respectively) showed the lowest ($p < 0.05$) affinity for water, with no statistical difference between them. These results are lower than those reported for blue, white, and hybrid (conventional source) corn starch, which showed values of 0.85 [19], but are higher than those reported by De Dios et al. [22] for starches from avocado seed cvs. Hass and Criollo (0.63) and by Wang et al. [17] for potato and sweet potato tuber starches (0.67 and 0.73, respectively).
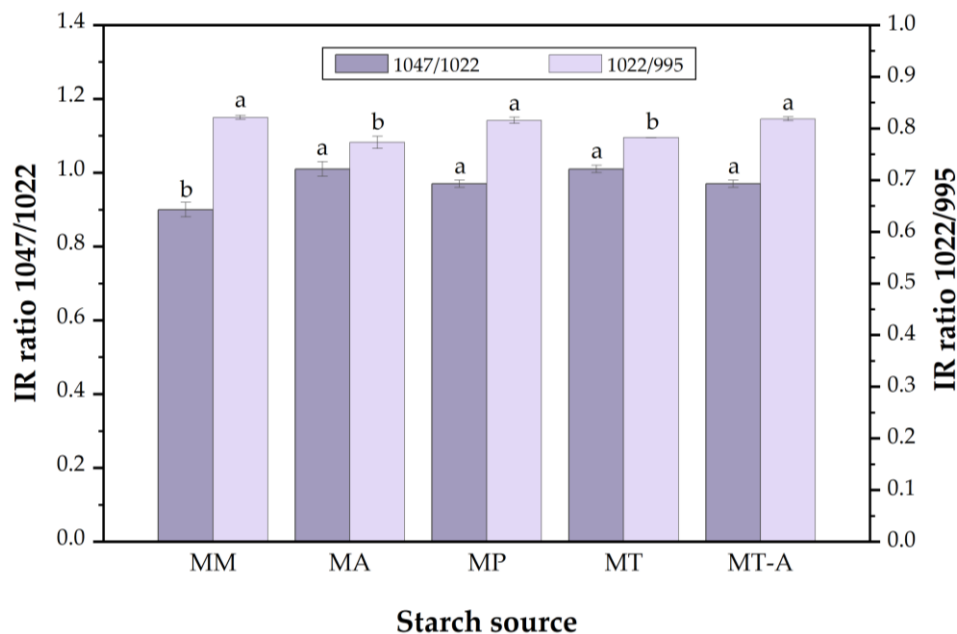
Figure 3. IR ratios of the absorbances 1047/1020 and 1022/995 cm^{-1} of mango seed starches. Different letters (a and b) in the bars with the same color are statistically different ($p \leq 0.05$). Cultivars: Ataulfo (MA), Manililla (MM), Piña (MP), Tapana (MT), and Tommy Atkins (MT-A).

3.4. Thermal Properties by DSC

The results of the DSC analysis of mango seed starches are presented in Table 2. The transition temperatures (T_o, T_p, and T_c) of the evaluated starches differed significantly among cultivars, whereas no differences were observed in the gelatinization enthalpy (ΔH_{gel}).

Table 2. Thermal variables of mango seed starches.

Gelatinization Temperature	Cultivar				
	MA	**MM**	**MP**	**MT**	**MT-A**
T_o (°C)	71.92 ± 0.18 [d]	73.32 ± 0.07 [c]	78.06 ± 0.05 [a]	77.75 ± 0.07 [a]	74.59 ± 0.09 [b]
T_p (°C)	77.04 ± 0.19 [c]	77.44 ± 0.07 [c]	81.64 ± 0.09 [a]	81.87 ± 0.11 [a]	79.06 ± 0.18 [b]
T_c (°C)	84.30 ± 0.38 [c]	84.19 ± 0.38 [c]	87.16 ± 0.13 [a,b]	88.55 ± 0.38 [a]	86.45 ± 0.51 [b]
ΔH_{gel} (J/g)	11.36 ± 0.47 [a]	11.08 ± 0.67 [a]	11.71 ± 0.23 [a]	11.11 ± 0.28 [a]	11.86 ± 0.54 [a]

Values represent the mean ± standard error. Means in the same line with different superscript letters (a–d) are statistically different ($p \leq 0.05$). T_o = gelatinization onset temperature; T_p = peak gelatinization temperature; T_c = conclusion gelatinization temperature; ΔH_{gel} = gelatinization enthalpy. Cultivars: Ataulfo (MA), Manililla (MM), Piña (MP), Tapana (MT), and Tommy Atkins (MT-A).

MP and MT starches showed a T_o of 78.06 and 77.75 °C, respectively, significantly higher than the rest of the starches evaluated. On the other hand, the lowest T_o was presented by MA starch with 71.92 °C. The onset temperature represents the beginning of gelatinization and is closely related to granule swelling [19]. Low gelatinization onset temperatures could have important industrial implications because companies justify the cost of their processes, so lower temperatures and energy will be needed for gel formation [56]. These T_o values exceed those Patiño et al. [39] reported for immature mango seed starch (69.89 °C), but they are within the range of those reported for mango seed starches (T_o = 74.4–76.3 °C) [12]. On the other hand, the peak (T_p) and final (T_c) temperatures for all sources evaluated ranged from 77.04 to 81.87 °C and 84.19 to 88.55 °C,

respectively. These are within the range of those observed for other mango cultivars, which ranged from 75 to 86 °C [12,39].

In general, gelatinization temperatures of mango starches were high (71.92–88.55 °C), similar to those recorded for non-conventional sources such as jackfruit (*Artocarpus heterophyllus* Lam.) seed starches by presenting temperatures ranging from 71 to 89 °C [57,58]. In general, starches with high apparent amylose contents tend to show higher final gelatinization temperatures than other starches due to the presence of intermediate components (they are amylose-like molecules but present branched structures with longer branching chain lengths than amylopectin) [58,59]. In contrast, compared to the reported present research, conventional starch sources', such as corn and wheat, gelatinization temperatures are lower (65–79 and 53–66 °C, respectively) [19,60].

Concerning the enthalpy of gelatinization, no significant differences were observed in all the samples, which ranged from 11.08 to 11.86 J/g (Table 2). These results are higher than those Patiño et al. [39] reported for immature mango seed starch (9.04 J/g). The results indicate that starches absorbed more energy in the gelatinization process to break the crystalline arrangement of the granules [61].

3.5. X-Ray Diffraction (XRD)

Figure 4 shows the X-ray diffraction patterns of MA, MM, MP, MT, and MT-A starches. In general, all samples exhibited an A-type crystallinity pattern, with intense signals at angles (2θ) of 15° and 23° and two overlapping peaks at 17 and 18°. Tester and Debon [56] mention that A-type XRD patterns are characteristic of cereal starches; moreover, they are characterized by a high degree of packing (containing amylopectin chains of 23–29 glucose units), which makes them remarkably vulnerable to acid and enzyme attack, a key finding with potential implications for various industries [62]. These results are similar to those reported by several authors for mango seed starches of different cultivars, even with varying stages of fruit ripening [15,29,32,33]. According to Nayak et al. [48], mango starches with A-type patterns have excellent functional and thermal properties relevant to food applications and are employed in formulating biodegradable films.
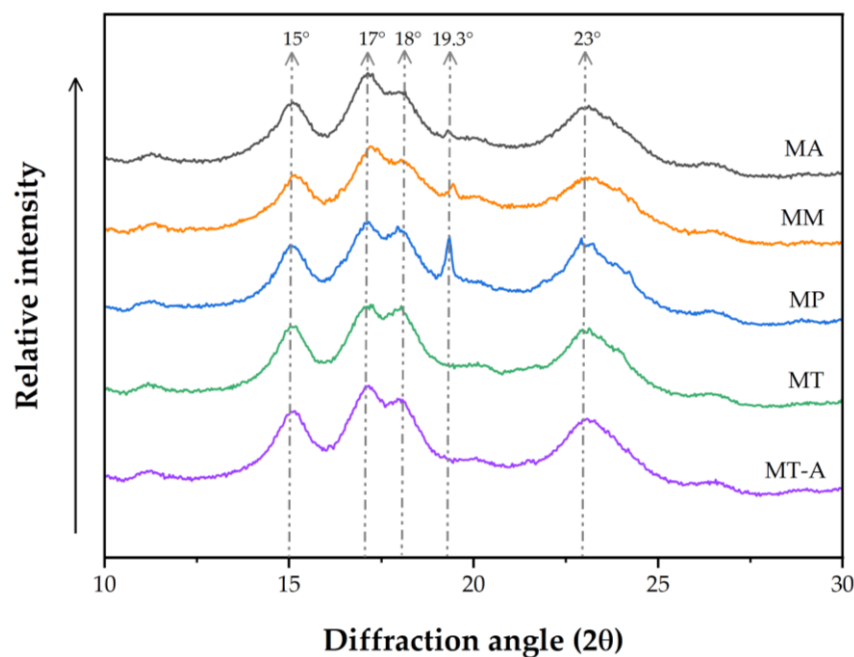

Figure 4. X-ray diffractogram of mango seed starches. Cultivars: Ataulfo (MA), Manililla (MM), Piña (MP), Tapana (MT), and Tommy Atkins (MT-A).

On the other hand, the diffraction patterns of MA, MM, and MP starches present a low-intensity signal in the angle (2θ) at 19.3°. These results are similar to those found by Patiño et al. [39] in immature mango starch, which are attributed to the presence of lipid–amylose complexes, suggesting the presence of stearic and palmitic acids in mango seed. Therefore, this lipid–amylose complex makes it more resistant to hydrolysis and generates resistant starch type 5, which makes it important for food and drug formulation [63].

3.6. Functional Properties

Figure 5 report the values for the swelling power (SP) and percent solubility (%P) of mango seed starches, respectively. As can be seen in Figure 5, both properties are directly correlated with temperature increases. The SP is related to the ability of the granules to retain water through hydrogen bonds, which is influenced by the content of amylose and amylopectin side chains [26]. Figure 5a shows the SP results evaluated at 60 °C, ranging from 1.98–2.29 g/g. Samples of MA and MM recorded the highest values ($p < 0.05$) (2.28 and 2.29 g/g, respectively), presenting no significant differences between them ($p > 0.05$). These values are similar to those reported by Mendes et al. [35] and Souza et al. [15], who observed values close to 1.90 g/g for starches from mango cv. Tommy Atkins at 65 °C. These results reveal that starches obtained from mango seeds present low SP at 60 °C, compared to starches from non-conventional sources such as Pitomba (*Talisia esculenta* Radlk.) (3.51 g/g) [64] and avocado (3.6 g/g) seeds [22].

The SP values also increased from 60 to 70 °C after increasing the temperature. The SP values ranged from 2.35 to 3.94 g/g, where MA and MM starches presented the highest swelling power (3.94 and 3.66 g/g, respectively), with no significant differences. The MT-A starch (3.37 g/g) presented lower ($p < 0.05$) SP than MA starch but was statistically equal ($p > 0.05$) to MM starch. Finally, MP and MT starches presented the lowest values ($p < 0.05$) for SP (2.64 and 2.35 g/g, respectively), with no significant differences ($p < 0.05$) between them. These results are lower than those reported by Mendes et al. [35] and Rodrigues et al. [13] for cv. Tommy Atkins starches (from 6.0 to 9.39 g/g at 75 °C). In a recent study, Jia et al. [65] pointed out that starch granules present limited SP when the temperature is below their T_p. However, when exceeding it, their water absorption capacity increases dramatically. In this regard, de Castro et al. [64] suggest that this behavior can be attributed to the fact that during the increase in temperature, a greater vibration of the molecules is promoted, causing the rupture of intermolecular bonds, allowing the released binding sites to form hydrogen bonds with the water molecule and thus increasing its water absorption capacity. This trend was verified when the temperature increased to 80 °C (Figure 5a), observing a drastic increase in SP values for all samples ($p < 0.05$). The highest values ($p < 0.05$) in SP were observed in samples of MM and MT-A (9.65 and 8.96 g/g, respectively), with no statistical difference detected between them ($p > 0.05$). On the other hand, MA starch presented lower SP (8.28 g/g) than MM starch ($p < 0.05$) but behaved statistically the same as MT-A starch. Finally, the lowest values at the evaluated temperature were observed for MP (7.51 g/g) and MT (7.67 g/g) starches, with no statistical difference between the two samples. These results were similar to those Souza et al. [15] for starch from mango cv. Tommy Atkins (≈9.4 g/g) but lower than those Bello-Pérez et al. [38] observed for starches from mango seeds cvs. Criollo (≈20 g/g) and Manila (≈23.5 g/g).

On the other hand, the percentage solubility of starches is related to the level of structural degradation of the granules. In addition, it can be influenced by several factors, such as particle size, amylose content, and degree of branching of the amylopectin chains. Figure 5b shows the %S of mango starches evaluated at different temperatures. The results observed at 60 °C revealed the MP starch presented the highest value ($p < 0.05$) in %S (1.60%), with no significant differences observed among the rest of the starches, with %S ranging from 0.64 to 0.84%. The solubility percentage presented the same behavior as SP after the increase in temperature from 60 to 70 °C; the solubility values increased slightly from 0.64–1.60 to 0.83–2.26%, respectively. However, when reaching a temperature of 80 °C the %S values increased rapidly, with MA starch (7.98%) presenting the highest solubility

($p < 0.05$), followed by MM, MT, and MT-A starches (5.81, 5.48, and 6.24%, respectively), with no significant difference detected among them. At this temperature, the lowest solubility ($p < 0.05$) was recorded for MP starch (3.07%). This tendency can be attributed to the fact that during heating of the granules in excess moisture at a temperature close to their T_p, the granules lose their structural integrity, promoting the solubilization of amylose chains and, in minor grade, the amylopectin [15].
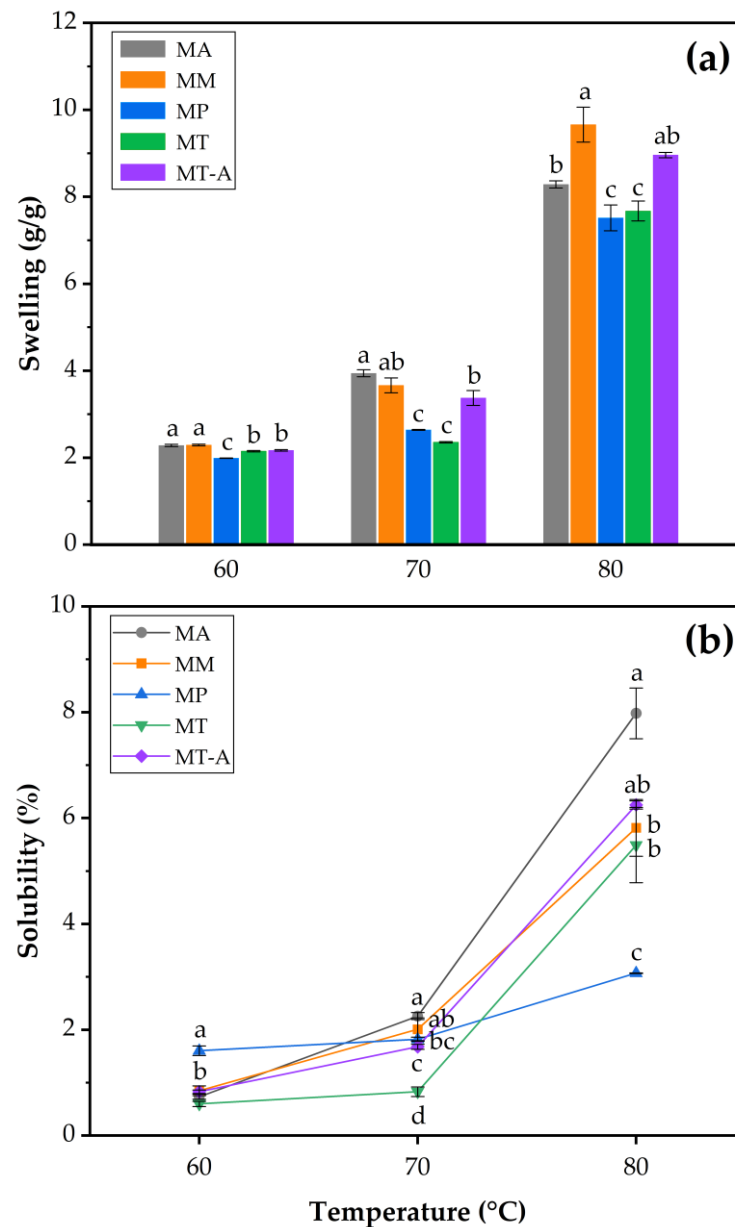

Figure 5. Functional properties of mango seed starches. (**a**) Swelling power (SP); (**b**) percent water solubility (%S). Values represent the mean ± standard error. Means with different letters (a–d) within the same temperature are statistically different ($p \leq 0.05$). Cultivars: Ataulfo (MA), Manililla (MM), Piña (MP), Tapana (MT), and Tommy Atkins (MT-A).

In general, the results of the present work evidenced that the functional properties of mango seed starches, such as SP and %S from the same botanical source, are influenced by the type of cultivars. These properties depend on the molecular structure of amylose and amylopectin, granule size, and amylose/amylopectin ratio [12,13,15,48]. Therefore, further studies are needed to help describe these characteristics of the starches analyzed in the present research.

3.7. Rheological Properties

3.7.1. Flow Curves

The flow curves of the mango seed starches are shown in Figure 6. The shear stress curves as a function of shear rate evidenced that all gelatinized starch samples exhibited a non-Newtonian behavior. The flow curves were fitted to the power law model ($R^2 > 0.99$), and the flow behavior index (n) and consistency index (k) were obtained (Table 3). The results show that all gelatinized starches from mango seeds presented $n < 1$, characteristic of "shear-thinning" fluids known as pseudoplastics. The n values presented significant differences ($p < 0.05$) ranging between 0.32 and 0.56. These results were greater than those observed by Casarrubias-Castillo et al. [66] in starches from barley (0.23), corn (0.17), mango (0.16), and banana (0.22).
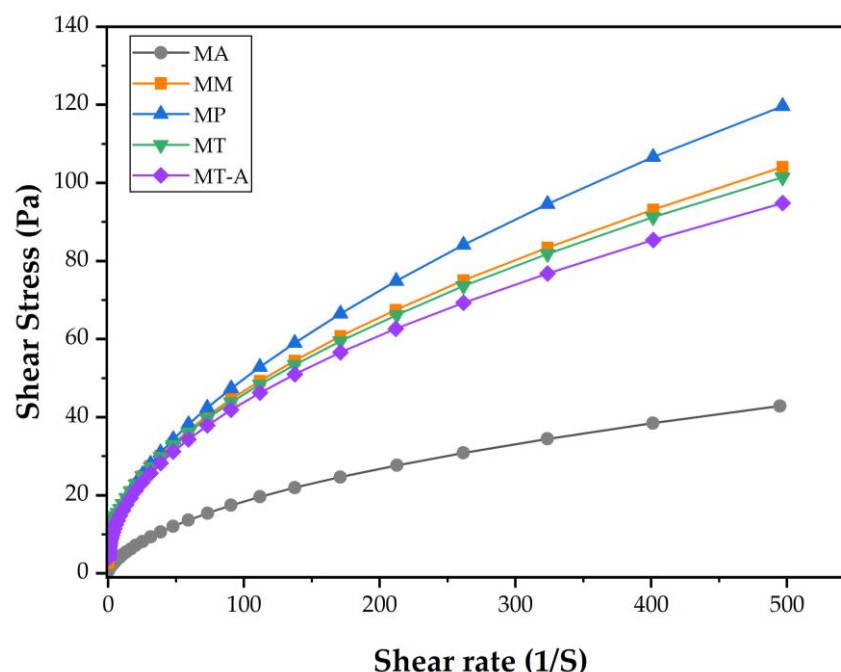

Figure 6. Variation of shear stress as a function of shear rate of mango seed starches. Cultivars: Ataulfo (MA), Manililla (MM), Piña (MP), Tapana (MT), and Tommy Atkins (MT-A).

Table 3. Rheological variables of mango seed starches obtained by the potential law model ($\tau = K\gamma^n$).

Source	n	k (Pa $\times$ s^n)	R^2
MA	0.56 ± 0.01 [a]	1.32 ± 0.09 [d]	0.992 ± 0.00 [a,b]
MM	0.43 ± 0.01 [b]	6.51 ± 0.20 [c]	0.997 ± 0.00 [a,b]
MP	0.39 ± 0.00 [c]	8.12 ± 0.14 [b]	0.983 ± 0.00 [c]
MT	0.32 ± 0.00 [d]	10.39 ± 0.00 [a]	0.961 ± 0.00 [d]
MT-A	0.39 ± 0.00 [c]	7.05 ± 0.06 [c]	0.990 ± 0.00 [b]

Values represent the mean ± standard error. Means in the same column with different superscript letters (a–d) are statistically different ($p \leq 0.05$). n: flow behavior index, k: consistency index. R^2: coefficient of determination. Cultivars: Ataulfo (MA), Manililla (MM), Piña (MP), Tapana (MT), and Tommy Atkins (MT-A).

According to the n values (Table 3), the starches followed the following decreasing order ($p < 0.05$) in their flow tendency: MA > MM > (MP = MT-A) > MT. The MA starch presented a higher flow index (0.56); this may be related to its high apparent amylose content (47.58%, Table 1). On the other hand, MT starch presented lower values of n (0.32) despite its high apparent amylose content (35.7%). The shear flow behavior is related to the progressive orientation of the molecules in the flow direction and the rupture of the hydrogen bonds formed in the amylose–amylopectin–water structure during shear. Therefore, compared to the other cultivars, the MT starch exhibited a slightly smoother

flow pattern, probably due to the formation of weaker bonds between the chains [67]. Gałkowska et al. [68] have previously reported this behavior during the behavior of the flow properties of corn and potato starches.

Regarding the consistency index (k), values varied significantly ($p < 0.05$) and ranged from 1.32 to 10.39 Pa $\times$ s^n (Table 3) with the following descending order: MT > MP > (MM = MT-A) > MA. These results are within the range reported for starches from different mango cultivars (Tommy Atkins, Totapuri, Nawdokmai, and Kaew) evaluated by viscoamylograph and rheometry, with values ranging from 0.192 to 14.42 Pa $\times$ s^n [15,16,31,48].

The consistency index is an analogy of viscosity, which determines the thickening power of starch for various applications [59]. According to the theory of Hoover and Vasanthan [69], the leaching of swollen starch granules during the gelatinization process also influences the viscosity of starches. The apparent amylose content reported in Table 1 was greater in MT starch (35.7%) than in MT-A and MP starches (32.6 and 25.6%, respectively), which could explain the higher values of k for MT starch (10.39 Pa $\times$ s^n) (Table 3). However, in MA and MM starches, their k values (1.32 and 6.51 Pa $\times$ s^n, respectively) cannot be correlated with this theory since the amount of amylose is quite comparable (47.5 and 31.6%, respectively). However, this behavior could be attributed to the relatively high lipid content of MM and MA starch (0.053%, Table 1). These components form lipid-soluble complexes, preventing water penetration into the granules during gelatinization. Similar behavior was reported by Saeaurng and Kuakpetoon [16] concerning Indian mango starch cultivars Namdokmai, Kaew, and Chokanan, with similar amylose and lipid contents (0.53–0.55 and 31.5–33.1%, respectively).

On the other hand, anomalous amylopectin (intermediate material between amylose and amylopectin) has been reported in starches with an A-type crystalline pattern [70]. According to Hoover and Vasanthan [71], anomalous amylopectin tends to be co-lixiviated with amylose during gelatinization. Since the differences in swelling factor and amylose leaching between MA and MM starches were marginal (1.32 and 6.51 Pa $\times$ s^n, respectively), it could suggest that anomalous amylopectin is present in the continuous matrix of MM starch to a greater extent compared to MA starch. In this sense, the present study requires further study of the composition of these portions to determine the implications of this behavior.

3.7.2. Viscoelastic Tests

According to Punia et al. [72], the dynamic viscoelastic properties reveal the ability of starches to form pastes or gels. Therefore, these properties are assessed under a wide temperature range since products with starch in their formulation are subjected to different temperatures during processing and storage. The storage modulus (G′) refers to the strain energy recovered per deformation cycle and reflects the elastic nature of the gel. In contrast, the loss modulus (G″) measures the energy dissipated as heat per deformation cycle, better known as the viscous modulus [72]. The relation G″/G′ represents the tan δ, also called the loss factor. When the tan δ recorded small values (δ < 1, G′ is greater than G″), the deformation is essentially recoverable, and the gels are rigid, behaving like a solid. In comparison, if tan δ > 1 (G′ is less than G″), the energy used to deform the gel is mainly dissipated; the material is less rigid, behaving more like a liquid [59].

The changes in the storage modulus (G′) and loss modulus (G″) of gels of mango seed starches during heating are shown in Figure 7. In all cases, a progressive increase in the values of G′ and G″ is observed until reaching a maximum value (G′$_{max}$ and G″$_{max}$) as a consequence of swollen starch granules and leaching of amylose chains, which promote the formation of a composite network of solvated materials supporting partially disintegrated starch granules [30,73]. As the temperature increases, G′ and G″ decrease gradually due to greater mobility, breaking the network by rupturing bond hydrogens, other molecular forces, and swollen starch granules [14,74].
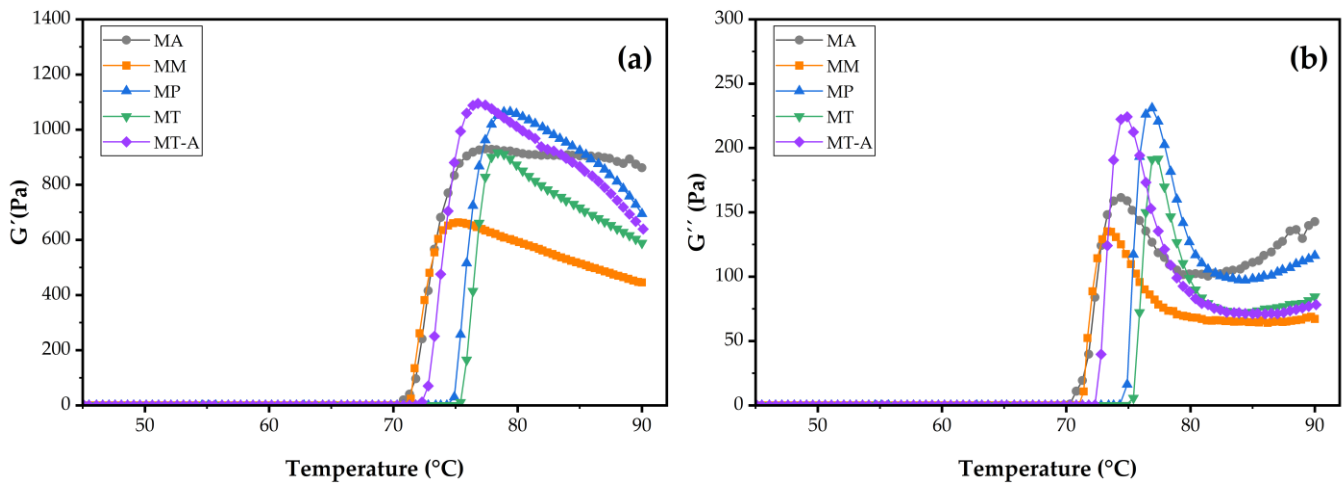
Figure 7. Changes in (**a**) storage modulus (G′) and (**b**) loss modulus (G″) of mango seed starches during heating. Cultivars: Ataulfo (MA), Manililla (MM), Piña (MP), Tapana (MT), and Tommy Atkins (MT-A).

Table 4 shows the dynamic rheological properties of starches isolated from mango seeds of different cultivars during temperature sweep testing. The temperature TG'_{max}, where the G′ reached a maximum value, ranged from 75.37 to 79.23 °C, showing significant differences ($p < 0.05$) among the five cultivars studied in the following order: (MP = MT) > MA > (MM = MT-A). These results are lower than those reported for mango seed starches (TG'_{max} = 82.4–89.4 °C) [2,14,30]. These results suggest that the mango seed starches of the present study are less resistant to heat and mechanical shearing. Therefore, they are more susceptible to viscosity losses [19]. This behavior is attributed to the degree of parallel packing of the adjacent double helices of the granules [50]. In this regard, Vamadevan et al. [75] mention that a long chain length between blocks facilitates their parallel packing, resulting in high gelatinization temperatures, while a short chain contributes to a less ordered alignment of the double helices; thus, they tend to present low temperatures. In general, the TG'_{max} results obtained from the viscoelastic tests are similar to the peak gelatinization temperatures (T_p) determined during thermal analysis by DSC (Table 2).

Table 4. Dynamic rheological properties of mango seed starches during heating.

Source	TG'_{max} (°C)	G'_{max} (Pa)	G″ (Pa)	tan δ G'_{max}
MA	76.95 ± 0.26 [b]	933.2 ± 2.08 [b]	158.85 ± 1.53 [c]	0.13 ± 0.00 [b]
MM	75.37 ± 0.17 [c]	650.9 ± 7.68 [c]	135.15 ± 2.54 [c]	0.16 ± 0.00 [a]
MP	79.23 ± 0.17 [a]	1066.33 ± 27.55 [a]	231.06 ± 8.80 [a]	0.14 ± 0.01 [a,b]
MT	78.40 ± 0.29 [a]	918.70 ± 18.05 [b]	191.96 ± 7.60 [b]	0.16 ± 0.01 [a]
MT-A	76.73 ± 0.23 [c]	1123.67 ± 16.18 [a]	213.46 ± 5.43 [a,b]	0.14 ± 0.01 [ab]

Values represent the mean ± standard error. Means in the same column with different superscript letters (a–c) are statistically different ($p \leq 0.05$). Cultivars: Ataulfo (MA), Manililla (MM), Piña (MP), Tapana (MT), and Tommy Atkins (MT-A).

The maximum values for modulus G′ and G″ (G'_{max} and G''_{max}, respectively) are shown in Table 4. It is evident that all the samples evaluated presented more elastic than viscous behavior (G′ > G″). This behavior agrees with what has been reported for starches from various botanical sources, including mango seed starch [14,19,22]. According to Chel et al. [76], this characteristic can be used as an additive in the food industry in gel-type products, such as baby food, sauces, and jellies, providing a soft texture and remaining soft even at low temperatures.

The G'_{max} and G''_{max} of mango starches ranged from 650.90 to 1123.67 Pa and 135.15 to 231.06 Pa, respectively (Table 4). The G'_{max} values varied significantly ($p < 0.05$) and presented the following descending order: (MP = MT-A) > (MA = MT) > MM. Meanwhile, the G''_{max} values followed this decreasing order: (MP = MT-A) > MT > (MA = MM). These differences may vary depending on factors such as starch type, high polymorphic diversity among cultivars, amylose/amylopectin ratio, starch concentration in the suspension, pH, and presence/concentration of other compounds [77,78]. However, these results are similar to those reported by Thory and Sandhu [14] for mango starch gels (G' = 1396 Pa, G'' = 162 Pa) at a concentration of 15% (w/w).

The tan δ values of the gels during heating (Table 4) ranged from 0.13 to 0.16 and are considered weak gels. According to the polymeric classification, gels obtained from amylaceous materials tend to present tan δ values close to zero [79]. This behavior is in agreement with that reported for starches from various botanical sources, such as corn (0.19–0.24) [19], avocado (0.18–0.21) [22], and even mango seed starch (0.11–0.38) [12,14]

4. Conclusions

Mango seeds of the cultivars Piña, Tapana, Manila, Ataulfo, and Tommy Atkins are a potential source for obtaining low-cost, high-yielding starch with promising characteristics for use in different industries. In this sense, the revalorization of these residues can contribute to the FAO Sustainable Development Goal 12, "Responsible production and consumption", to achieve sustainable management and efficient use of resources through revalorization activities. For this reason, to suggest possible applications of mango seed starches, it is essential to know the characteristics and properties of each cultivar. All starches evaluated showed significant differences in physicochemical, morphological, molecular, thermal, and rheological properties. Tommy Atkins mango seed starch had the highest yield and amylose content than other cultivars.

On the other hand, it is important to note that the wet milling extraction method with alkaline solutions resulted in higher purity starches by reducing the ash, lipid, and protein content. On the other hand, the wet milling extraction method with alkaline solutions resulted in higher purity starches by reducing the ash, lipid, and protein content. Despite this, it is necessary to mention that in some sources, such as Ataulfo mango, pineapple, and Tommy Atkins, its application generated granules with slight surface damage, such as cracks and porous regions. However, these characteristics could improve their digestibility, texture, solubility, and gelling capacity, a desirable attribute in the formulation of food products. On the other hand, all the samples presented a more elastic than viscous behavior, a desirable attribute in the formulation of soft-textured products at low temperatures. Regarding the thermal analysis, the results indicate that the transition temperatures were higher than those of conventional sources. In general, mango seed starches from the different cultivars evaluated have potential for use in the food industry, especially in the formulation of baby food, sauces, and bakery products.

Conflicts of Interest: The authors declare that they have no known competing financial interests or personal relationships that could have appeared to influence the work reported in this paper.

References

1. SAGARPA. Servicio de Información Agroalimentaria y Pesquera. Available online: https://nube.siap.gob.mx/cierreagricola/ (accessed on 30 April 2024).
2. Punia, B.S.; Kumar, M.; Whiteside, W.S. Mango seed starch: A sustainable and eco-friendly alternative to increasing industrial requirements. *Int. J. Biol. Macromol.* **2021**, *183*, 1807–1817. [CrossRef] [PubMed]
3. Owino, W.O.; Ambuko, J.L. Mango fruit processing: Options for small-scale processors in developing countries. *Agriculture.* **2021**, *11*, 1105. [CrossRef]
4. Yatnatti, S.; Vijayalakshmi, D. Study of soup mix incorporated with starch extract from mango "*Mangifera indica*" seed kernels. *Curr. Res. Nutr. Food Sci.* **2018**, *6*, 816–825. [CrossRef]
5. Kittiphoom, S. Utilization of mango seed. *Int. Food Res. J.* **2012**, *19*, 1325–1335.
6. Lebaka, V.R.; Wee, Y.-J.; Ye, W.; Korivi, M. Nutritional composition and bioactive compounds in three different parts of mango fruit. *Int. J. Environ. Res. Public Health* **2021**, *18*, 741. [CrossRef]
7. El-Sanafawy, H.A.; Maggiolino, A.; El-Esawy, G.S.; Riad, W.A.; Zeineldin, M.; Abdelmegeid, M.; Seboussi, R.; EL-Nawasany, L.I.; Elghandour, M.M.M.Y.; De Palo, P.; et al. Effect of mango seeds as an untraditional source of energy on the productive performance of dairy Damascus goats. *Front. Vet. Sci.* **2023**, *10*, 1058915. [CrossRef]
8. Sultana, B.; Ashraf, R. Mango (*Mangifera indica* L.) seed oil. In *Fruit Oils: Chemistry and Functionality*; Ramadan, M.F., Ed.; Springer: Cham, Switzerland, 2019; pp. 561–575.
9. Correa, D.E.; Romero, B.M.; León, N. Extracción de taninos de semilla de mango criollo (*Mangifera indica* L.) y su aplicación como curtiente. *J. Agro–Ind. Sci.* **2019**, *1*, 51–55. [CrossRef]
10. Torres-León, C.; Rojas, R.; Serna-Cock, L.; Belmares-Cerda, R.; Aguilar, C.N. Extraction of antioxidants from mango seed kernel: Optimization assisted by microwave. *Food Bioprod. Process.* **2017**, *105*, 188–196. [CrossRef]
11. Torres-León, C.; de Azevedo Ramos, B.; dos Santos Correia, M.T.; Carneiro-da-Cunha, M.G.; Ramirez-Guzman, N.; Alves, L.C.; Brayner, F.A.; Ascacio-Valdes, J.; Álvarez-Pérez, O.B.; Aguilar, C.N. Antioxidant and anti-staphylococcal activity of polyphenolic-rich extracts from Ataulfo mango seed. *LWT* **2021**, *148*, 111653. [CrossRef]
12. Kaur, M.; Singh, N.; Sandhu, K.S.; Guraya, H.S. Physicochemical, morphological, thermal and rheological properties of starches separated from kernels of some Indian mango cultivars (*Mangifera indica* L.). *Food Chem.* **2004**, *85*, 131–140. [CrossRef]
13. Rodrigues, A.A.M.; Santos, L.F.D.; Costa, R.R.D.; Félix, D.T.; Nascimento, J.H.B.; Lima, M.A.C.d. Characterization of starch from different non-traditional sources and its application as coating in 'Palmer'mango fruit. *Ciênc. Agrotec.* **2020**, *44*, e011220. [CrossRef]
14. Thory, R.; Sandhu, K.S. A comparison of mango kernel starch with a novel starch from litchi (*Litchi chinensis*) kernel: Physico-chemical, morphological, pasting, and rheological properties. *Int. J. Food Prop.* **2017**, *20*, 911–921. [CrossRef]
15. Souza, J.C.A.d.; Macena, J.F.F.; Andrade, I.H.P.; Camilloto, G.P.; Cruz, R.S. Functional characterization of mango seed starch (*Mangifera indica* l.). *Res. Soc. Dev.* **2021**, *10*, e30310310118. [CrossRef]
16. Saeaurng, K.; Kuakpetoon, D. A comparative study of mango seed kernel starches and other commercial starches: The contribution of chemical fine structure to granule crystallinity, gelatinization, retrogradation, and pasting properties. *J. Food Meas. Charact.* **2018**, *12*, 2444–2452. [CrossRef]
17. Wang, H.; Yang, Q.; Gao, L.; Gong, X.; Qu, Y.; Feng, B. Functional and physicochemical properties of flours and starches from different tuber crops. *Int. J. Biol. Macromol.* **2020**, *148*, 324–332. [CrossRef]
18. Golea, C.M.; Galan, P.M.; Leti, L.I.; Codină, G.G. Genetic Diversity and physicochemical characteristics of different wheat species (*Triticum aestivum* L., *Triticum monococcum* L., *Triticum spelta* L.) cultivated in Romania. *Appl. Sci.* **2023**, *13*, 4992. [CrossRef]
19. Bustillos, R.J.C.; Tirado, G.J.M.; Ordonez, G.M.; Zamudio, F.P.B.; Ornelas, P.J.d.J.; Acosta, M.C.H.; Gallegos, M.G.; Páramo, C.D.E.; Rios, V.C. Physicochemical, thermal and rheological properties of three native corn starches. *Food Sci. Technol.* **2018**, *39*, 149–157. [CrossRef]
20. Kumar, Y.; Shikha, D.; Guzmán-Ortiz, F.A.; Sharanagat, V.S.; Kumar, K.; Saxena, D.C. Starch: Current Production and Consumption Trends. In *Starch: Advances in Modifications, Technologies and Applications*; Sharanagat, V.S., Saxena, D.C., Kumar, K., Kumar, Y., Eds.; Springer: Berlin/Heidelberg, Germany, 2023; pp. 1–10.
21. Burgaard, J. Sustainability Report 2021/22: A Circular Business Model. 2022. Available online: https://14541121.fs1.hubspotusercontent-na1.net/hubfs/14541121/KMC_CSR_2021_22_WEB_UK2.pdf?hsCtaTracking=489ba677-2c61-4d52-acce-3cc04285643c%7C49fa5e9b-3789-400c-8adf-a94886c21aae (accessed on 16 September 2024).
22. De Dios, A.N.; Tirado, G.J.M.; Rios, V.C.; Luna, E.G.; Isiordia, A.N.; Zamudio, F.P.B.; Estrada, V.M.O.; Cambero, C.O.J. Physico-chemical, structural, thermal and rheological properties of flour and starch isolated from avocado seeds of landrace and hass cultivars. *Molecules* **2022**, *27*, 910. [CrossRef]
23. Kushwaha, R.; Singh, V.; Kaur, S.; Kaur, D. Characterization and Comparative Analysis of Starches from Seeds of Five Jackfruit Cultivars. *Starch-Stärke* **2023**, *75*, 2200208. [CrossRef]

24. Tosif, M.M.; Bains, A.; Sadh, P.K.; Sarangi, P.K.; Kaushik, R.; Burla, S.V.S.; Chawla, P.; Sridhar, K. Loquat seed starch—Emerging source of non-conventional starch: Structure, properties, and novel applications. *Int. J. Biol. Macromol.* **2023**, *244*, 125230. [CrossRef]

25. Hardiyanti, R.; Suharman, S.; Sinaga, M.Z.E.; Mahendra, I.P.; Hartanto, A. Physicochemical characteristics of modified starch granules from *Durio zibethinus* Murr. var. Bintana. *AIP Conf. Proc.* **2021**, *2342*, 080007. [CrossRef]

26. Magallanes-Cruz, P.A.; Duque-Buitrago, L.F.; Martínez-Ruiz, N.d.R. Native and modified starches from underutilized seeds: Characteristics, functional properties and potential applications. *Food Res. Int.* **2023**, *169*, 112875. [CrossRef] [PubMed]

27. Ferreira, S.; Araujo, T.; Souza, N.; Rodrigues, L.; Lisboa, H.M.; Pasquali, M.; Trindade, G.; Rocha, A.P. Physicochemical, morphological and antioxidant properties of spray-dried mango kernel starch. *J. Agric. Res.* **2019**, *1*, 100012. [CrossRef]

28. Nayak, P.; Rayaguru, K. Studies on extraction of starch from dried and fresh mango seed kernel. *Int. J. Agr. Sci.* **2018**, *10*, 7192–7195.

29. Ferraz, C.A.; Fontes, R.L.; Fontes-Sant'Ana, G.C.; Calado, V.; López, E.O.; Rocha-Leão, M.H. Extraction, modification, and chemical, thermal and morphological characterization of starch from the agro-industrial residue of mango (*Mangifera indica* L) var. Ubá. *Starch-Stärke* **2019**, *71*, 1800023. [CrossRef]

30. Mieles, G.L.; Quintana, S.E.; García, Z.L.A. Ultrasound-assisted extraction of mango (*Mangifera indica*) kernel starch: Chemical, techno-functional, and pasting properties. *Gels* **2023**, *9*, 136. [CrossRef]

31. do Nascimento Marques, N.; do Nascimento Garcia, C.S.; Madruga, L.Y.C.; Villetti, M.A.; de Souza Filho, M.d.S.; Ito, E.N.; de Carvalho Balaban, R. Turning industrial waste into a valuable bioproduct: Starch from mango kernel derivative to oil industry mango starch derivative in oil industry. *J. Renewable Mater.* **2019**, *7*, 139. [CrossRef]

32. Cordeiro, E.M.S.; Nunes, Y.L.; Mattos, A.L.A.; Rosa, M.F.; de sá, M.; Sousa Filho, M.; Ito, E.N. Polymer biocomposites and nanobiocomposites obtained from mango seeds. *Macromol. Symp.* **2014**, *344*, 39–54. [CrossRef]

33. Shahrim, N.A.; Sarifuddin, N.; Ismail, H. Extraction and characterization of starch from mango seeds. *J. Phys. Conf. Ser.* **2018**, *1082*, 012019. [CrossRef]

34. Yadav, A.; Kumar, N.; Upadhyay, A.; Singh, A.; Anurag, R.K.; Pandiselvam, R. Effect of mango kernel seed starch-based active edible coating functionalized with lemongrass essential oil on the shelf-life of guava fruit. *Qual. Assur. Saf. Crop* **2022**, *14*, 103–115. [CrossRef]

35. Mendes, M.L.M.; Ribeiro, A.P.L.; Almeida, E.C. Efeito da acidificação nas propriedades físico-químicas e funcionais do amido de sementes de manga (*Mangifera indica* L.), variedade Tommy Atkins. *Rev. Ceres.* **2015**, *62*, 225–232. [CrossRef]

36. de Oliveira, M.A.L.; Madruga, L.Y.C.; de Lima, B.L.B.; Villetti, M.A.; de Souza Filho, M.S.M.; Kipper, M.J.; Marques, N.N.; Balaban, R.C. Agro-industrial waste valorization: Transformation of starch from mango kernel into biocompatible, thermoresponsive and high swelling nanogels. *J. Braz. Chem. Soc.* **2021**, *32*, 1607–1616. [CrossRef]

37. Gálvez, L.D.; Salvador, F.M.; Adriano, A.M.; Mayek, P.N. Morphological characterization of native mangos from Chiapas, Mexico. *Subtrop. Plant Sci.* **2010**, *62*, 18–26.

38. Bello-Pérez, L.A.; Aparicio-Saguilán, A.; MÉNdez-Montealvo, G.; Solorza-Feria, J.; Flores-Huicochea, E. Isolation and partial characterization of mango (*Magnifera indica* L.) Starch: Morphological, physicochemical and functional studies. *Plant Foods Hum. Nutr.* **2005**, *60*, 7–12. [CrossRef]

39. Patiño, R.O.; Agama, A.E.; Ramos, L.G.; Bello, P.L.A. Unripe mango kernel starch: Partial characterization. *Food Hydrocoll.* **2020**, *101*, 105512. [CrossRef]

40. AOAC (Association of Official Analytical Chemist). *Official Methods of Analysis of AOAC International*, 17th ed.; AOAC: Gaithersburg, MD, USA, 2002.

41. Williams, P.; Kuzina, F.; Hlynka, I. Rapid colorimetric procedure for estimating the amylose content of starches and flours. *Cereal Chem.* **1970**, *47*, 411–420.

42. Gunning, Y.M.; Gunning, P.A.; Kemsley, E.K.; Parker, R.; Ring, S.G.; Wilson, R.H.; Blake, A. Factors affecting the release of flavor encapsulated in carbohydrate matrixes. *J. Agric. Food Chem.* **1999**, *47*, 5198–5205. [CrossRef]

43. Tirado-Gallegos, J.; Zamudio-Flores, P.; Ornelas-Paz, J.d.J.; Rios-Velasco, C.; Acosta-Muñiz, C.; Gutiérrez-Meraz, F.; Islas-Hernández, J.; Salgado-Delgado, R. Efecto del método de aislamiento y el estado de madurez en las propiedades fisicoquímicas, estructurales y reológicas de almidón de manzana. *Rev. Mex. Ing. Quim.* **2016**, *15*, 391–408. [CrossRef]

44. Ye, J.; Liu, C.; Luo, S.; Hu, X.; McClements, D.J. Modification of the digestibility of extruded rice starch by enzyme treatment (β-amylolysis): An in vitro study. *Food Res. Int.* **2018**, *111*, 590–596. [CrossRef]

45. Sánchez-Rivera, M.M.; Almanza-Benitez, S.; Bello-Perez, L.A.; Mendez-Montealvo, G.; Núñez-Santiago, M.C.; Rodriguez-Ambriz, S.L.; Gutierrez-Meráz, F. Acetylation of banana (*Musa paradisiaca* L.) and corn (*Zea mays* L.) starches using a microwave heating procedure and iodine as catalyst: II. Rheological and structural studies. *Carbohydr. Polym.* **2013**, *92*, 1256–1261. [CrossRef]

46. Singh, N.; Inouchi, N.; Nishinari, K. Morphological, structural, thermal, and rheological characteristics of starches separated from apples of different cultivars. *J. Agric. Food Chem.* **2005**, *53*, 10193–10199. [CrossRef] [PubMed]

47. Tesfaye, T.; Johakimu, J.K.; Chavan, R.; Sithole, B.; Ramjugernath, D. Valorisation of mango seed via extraction of starch: Preliminary techno-economic analysis. *Clean Techn. Environ. Policy.* **2018**, *20*, 81–94. [CrossRef]

48. Nayak, P.; Rayaguru, K.; Brahma, S.; Routray, W.; Dash, S.K. Standardization of process protocol for isolation of starch from mango kernel and its characterization. *J. Sci. Food Agric.* **2022**, *102*, 2813–2825. [CrossRef] [PubMed]

49. Bharti, I.; Singh, S.; Saxena, D.C. Exploring the influence of heat moisture treatment on physicochemical, pasting, structural and morphological properties of mango kernel starches from Indian cultivars. *LTW* **2019**, *110*, 197–206. [CrossRef]

50. Zhu, K.; Yao, S.; Zhang, Y.; Liu, Q.; Xu, F.; Wu, G.; Dong, W.; Tan, L. Effects of in vitro saliva, gastric and intestinal digestion on the chemical properties, antioxidant activity of polysaccharide from *Artocarpus heterophyllus Lam.* (Jackfruit) pulp. *Food Hidrocoll.* **2019**, *87*, 952–959. [CrossRef]

51. Jhan, F.; Gani, A.; Noor, N.; Ashraf, Z.U.; Gani, A.; Shah, A. Characterisation and utilisation of nano-reduced starch from underutilised cereals for delivery of folic acid through human GI tract. *Sci. Rep.* **2021**, *11*, 4873. [CrossRef]

52. Dong, S.; Fang, G.; Luo, Z.; Gao, Q. Effect of granule size on the structure and digestibility of jackfruit seed starch. *Food Hydrocoll.* **2021**, *120*, 106964. [CrossRef]

53. Pelissari, F.M.; Andrade-Mahecha, M.M.; Sobral, P.J.d.A.; Menegalli, F.C. Isolation and characterization of the flour and starch of plantain bananas (*Musa paradisiaca*). *Starch-Stärke* **2012**, *64*, 382–391. [CrossRef]

54. Pozo, C.; Rodríguez-Llamazares, S.; Bouza, R.; Barral, L.; Castaño, J.; Müller, N.; Restrepo, I. Study of the structural order of native starch granules using combined FTIR and XRD analysis. *J. Polym. Res.* **2018**, *25*, 1–8. [CrossRef]

55. Sevenou, O.; Hill, S.; Farhat, I.; Mitchell, J. Organisation of the external region of the starch granule as determined by infrared spectroscopy. *Int. J. Biol. Macromol.* **2002**, *31*, 79–85. [CrossRef]

56. Tester, R.F.; Debon, S.J. Annealing of starch—A review. *Int. J. Biol. Macromol.* **2000**, *27*, 1–12. [CrossRef] [PubMed]

57. Juárez-Barrientos, J.M.; Hernández-Santos, B.; Herman-Lara, E.; Martínez-Sánchez, C.E.; Torruco-Uco, J.G.; de Jesus Ramírez-Rivera, E.; Pineda-Pineda, J.M.; Rodríguez-Miranda, J. Effects of boiling on the functional, thermal and compositional properties of the Mexican jackfruit (*Artocarpus heterophyllus*) seed Jackfruit seed meal properties. *Emir. J. Food Agric.* **2017**, *29*, 1–9. [CrossRef]

58. Zhang, Y.; Zhu, K.; He, S.; Tan, L.; Kong, X. Characterizations of high purity starches isolated from five different jackfruit cultivars. *Food Hydrocoll.* **2016**, *52*, 785–794. [CrossRef]

59. Ai, Y.; Jane, J.L. Gelatinization and rheological properties of starch. *Starch-Stärke* **2015**, *67*, 213–224. [CrossRef]

60. Shevkani, K.; Singh, N.; Bajaj, R.; Kaur, A. Wheat starch production, structure, functionality and applications—A review. *Int. J. Food Sci. Technol.* **2017**, *52*, 38–58. [CrossRef]

61. Li, C. Recent progress in understanding starch gelatinization—An important property determining food quality. *Carbohydr. Polym.* **2022**, *293*, 119735. [CrossRef]

62. Alqah, H.; Alamri, M.S.; Mohamed, A.A.; Hussain, S.; Qasem, A.A.; Ibraheem, M.A.; Ababtain, I.A. The effect of germinated sorghum extract on the pasting properties and swelling power of different annealed starches. *Polymers.* **2020**, *12*, 1602. [CrossRef]

63. Zhong, H.; She, Y.; Yang, X.; Wen, Q.; Chen, L.; Wang, X.; Chen, Z. Analysis of the mechanism of resistance to enzymatic hydrolysis of RS-5 resistant starch. *Food Chem.* **2024**, *452*, 139570. [CrossRef]

64. de Castro, D.S.; dos Santos Moreira, I.; de Melo Silva, L.M.; Lima, J.P.; da Silva, W.P.; Gomes, J.P.; de Figueirêdo, R.M.F. Isolation and characterization of starch from pitomba endocarp. *Food Res. Int.* **2019**, *124*, 181–187. [CrossRef]

65. Jia, R.; Cui, C.; Gao, L.; Qin, Y.; Ji, N.; Dai, L.; Wang, Y.; Xiong, L.; Shi, R.; Sun, Q. A review of starch swelling behavior: Its mechanism, determination methods, influencing factors, and influence on food quality. *Carbohydr. Polym.* **2023**, *321*, 121260. [CrossRef]

66. Casarrubias-Castillo, M.G.; Méndez-Montealvo, G.; Rodríguez-Ambriz, S.L.; Sánchez-Rivera, M.M.; Bello-Pérez, L.A. Structural and rheological differences between fruit and cereal starches. *Agrociencia* **2012**, *46*, 455–466.

67. Moreira, R.; Chenlo, F.; Torres, M.; Glazer, J. Rheological properties of gelatinized chestnut starch dispersions: Effect of concentration and temperature. *J. Food Eng.* **2012**, *112*, 94–99. [CrossRef]

68. Gałkowska, D.; Pycia, K.; Juszczak, L.; Pająk, P. Influence of cassia gum on rheological and textural properties of native potato and corn starch. *Starch-Stärke* **2014**, *66*, 1060–1070. [CrossRef]

69. Hoover, R.; Vasanthan, T. The flow properties of native, heat-moisture treated, and annealed starches from wheat, oat, potato and lentil. *J. Food Biochem.* **1994**, *18*, 67–82. [CrossRef]

70. Paton, D. Oat starch: Some recent developments. *Starch-Stärke* **1979**, *31*, 184–187. [CrossRef]

71. Hoover, R.; Vasanthan, T. Studies on isolation and characterization of starch from oat (*Avena nuda*) grains. *Carbohydr. Polym.* **1992**, *19*, 285–297. [CrossRef]

72. Punia, S.; Sandhu, K.S.; Dhull, S.B.; Siroha, A.K.; Purewal, S.S.; Kaur, M.; Kidwai, M.K. Oat starch: Physico-chemical, morphological, rheological characteristics and its applications—A review. *Int. J. Biol. Macromol.* **2020**, *154*, 493–498. [CrossRef]

73. Chen, N.; Wang, Q.; Wang, M.-X.; Li, N.-Y.; Briones, A.V.; Cassani, L.; Prieto, M.A.; Carandang, M.B.; Liu, C.; Gu, C.-M.; et al. Characterization of the physicochemical, thermal and rheological properties of cashew kernel starch. *Food Chem. X* **2022**, *15*, 100432. [CrossRef]

74. Zhang, L.; Wang, X.; Li, S.; Sun, J.; Liu, X. Effect of inulin on the pasting, textural, and rheological properties of sweet potato starch. *CYTA J. Food* **2019**, *17*, 733–743. [CrossRef]

75. Vamadevan, V.; Bertoft, E.; Seetharaman, K. On the importance of organization of glucan chains on thermal properties of starch. *Carbohydr. Polym.* **2013**, *92*, 1653–1659. [CrossRef]

76. Chel, G.L.; Barbosa, M.E.; Martínez, A.A.; González, M.E.; Betancur, A.D. Some physicochemical and rheological properties of starch isolated from avocado seeds. *Int. J. Biol. Macromol.* **2016**, *86*, 302–308. [CrossRef] [PubMed]

77. Choi, H.M.; Yoo, B. Rheology of mixed systems of sweet potato starch and galactomannans. *Starch-Stärke* **2008**, *60*, 263–269. [CrossRef]

78. Hagenimana, A.; Pu, P.; Ding, X. Study on thermal and rheological properties of native rice starches and their corresponding mixtures. *Food Res. Int.* **2005**, *38*, 257–266. [CrossRef]

79. Ferry, J.D. *Viscoelastic Properties of Polymers*, 3rd ed.; John Wiley & Sons: New York, NY, USA, 1980.